Quantum Electronics **50** (4) 321–326 (2020)

https://doi.org/10.1070/QEL17289

Ytterbium laser system for studying parametric amplification of femtosecond pulses with a centre wavelength of ~2 μm

I.B. Mukhin, M.R. Volkov, I.A. Vikulov, E.A. Perevezentsev, O.V. Palashov

Abstract. **A laser system is developed with an optical synchronisation of a femtosecond signal with a pump channel. The signal of a driving ytterbium fibre laser with a 60 MHz repetition rate of stretched femtosecond pulses is amplified in energy from several nanojoules to 0.4 mJ at a pulse repetition rate of 3 kHz in a wideband amplifier and then is compressed in time to 250 fs. The obtained radiation is used for generating femtosecond laser pulses with a centre wavelength of ~2 μm, pulse energy of above 20 μJ, duration of several field oscillations, and phase stabilisation between the electromagnetic field and envelope. The other pulse of the driving fibre laser provides optical synchronisation and a minimal time delay and is directed to a regenerative Yb:YAG disk amplifier for amplification to an energy of 4 mJ at a pulse repetition rate of 3 kHz and duration of 20 ps. A multipass disk amplifier is developed for further increasing the energy of pump chirped pulses to an energy of 70 mJ at a pulse repetition rate of 10 Hz and duration of 400 ps for studying parametric amplification under sub-nanosecond pumping.**

Keywords: *ytterbium fibre laser, femtosecond pulses, Yb:YAG disk amplifier, pulse compression, parametric amplification.*

1. Introduction

The development of laser sources with an extremely high peak radiation power in the IR range is one of the most promising fields in studying interaction of radiation with matter. At present, such sources have numerous scientific and technical applications. For example, in high-harmonic generation, a photon energy increases with a wavelength of initial radiation [1], and phase stabilisation between an electromagnetic field and envelope allows one to generate separated attosecond pulses [2]. A ponderomotive force increases with a wavelength, which results in more efficient electron acceleration [3]. The efficiency of generating terahertz radiation increases with a wavelength of incident femtosecond laser radiation as λ^5 [4], and the spectral width may reach several octaves. For now, we know only two laser installations of multi-terawatt power level operating in the IR spectral range [5, 6], both of those include a high-intensity Ti:sapphire laser for pumping a parametric amplifier. Such a system is not optimal, because for this purpose one can use ytterbium picosecond lasers [7, 8], which have a high pulse energy at a pulse repetition rate (PRR) of dozens and hundreds of hertz and are cheaper and simpler in use. A possibility of this approach is demonstrated, for example, in [9]. The present work reports first results on developing a laser system for studying parametric amplification of femtosecond pulses with a centre wavelength of ~2 μm pumped by picosecond pulses of ytterbium laser.

A flowchart of the laser system is given in Fig. 1. As a single radiation source, a commercial sub-picosecond ytterbium laser is used, comprised of a fibre source with a 60-MHz PRR and amplifier of pulses to an energy of 0.3 mJ with a PRR of up to 15 kHz and duration of 250 fs. The amplified signal is used for generating a wideband femtosecond radiation in the range of 2 μm basing on approaches similar to those in [9, 10]. In this case, the pumping is performed by another radiation pulse with a PRR of 60 MHz passed through the developed ytterbium disk amplifiers with an output energy of dozens of millijoules. Such a system provides optical synchronisation of the femtosecond pulse with the pump pulse. By choosing properly (from a series of pulses with a PRR of 60 MHz) the pulse amplified in the disk amplifiers, one can minimise a length of the delay line needed for synchronisation. Then the femtosecond radiation and pump radiation pass to the developed units of parametrical amplification and diagnosis of the parameters of amplified radiation

2. Pumping based on ytterbium disk amplifiers

For studying parametric amplification, two ytterbium disk amplifiers were elaborated with different output parameters. The first one is a regenerative Yb:YAG disk amplifier with a nanojoule-level input signal. A laser head used in the amplifier is described in [11], where the main characteristics of laser oscillation are given and high efficiency is demonstrated. Radiation of a sub-picosecond laser with a PRR of 60 MHz, bandwidth of ~10 nm, and pulse duration of 200 ps is directed to a regenerative amplifier, whose schematic is shown in Fig. 2. A Faraday isolator provides optical isolation between input and output radiation. A Pockels cell (PC) with water cooling of a BBO electro-optical crystal (with an aperture of 4 mm) and trigger time of 15 ns changes the Q-factor of the cavity with a disk active element (AE), thus realising the regenerative operation regime. A diameter of the pump beam on the AE disk is 3.5 mm (according to [12], the optimal diameter of the signal on AE is 0.75 that of the pump beam). The cavity of the regenerative amplifier (Fig. 2b) was calculated issuing from these parameters. The cavity round-trip length was 6 m, which corresponds to ~20 ns and is longer than the PC trigger time. Calculations of the fundamental mode take into account

I.B. Mukhin, M.R. Volkov, I.A. Vikulov, E.A. Perevezentsev, O.V. Palashov Institute of Applied Physics, Russian Academy of Sciences, ul. Ulyanova 46, 603950 Nizhny Novgorod, Russia; e-mail: mib_1982@mail.ru; bearuck@mail.ru

Received 19 February 2020
Kvantovaya Elektronika **50** (4) 321–326 (2020)
Translated by N.A. Raspopov

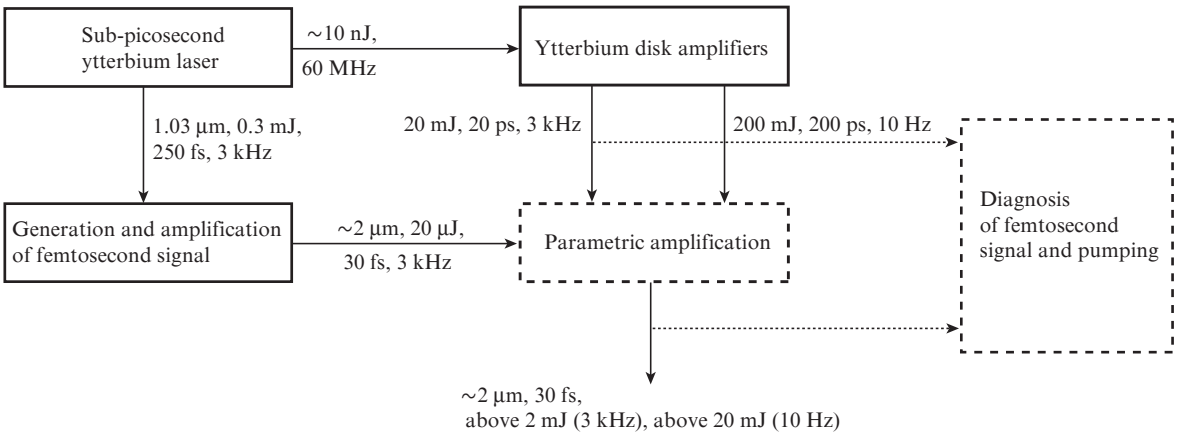

Figure 1. Flowchart of the laser system. Dotted lines refer to the units to be developed in the future.

the fact that the AE disk has a parabolic component in the phase profile [13], which is equivalent to a thin positive lens with a focal length of 9 m. However, the influence of the induced thermal lens on the optimal cavity geometry was neglected, because the optical power of such a lens is, as a rule, $\sim 10^{-3}$ m^{-1} [14]. The optical cavity with a disk AE was tested in cw lasing mode; over the entire range of the pump power, the beam quality parameter was $M^2 \leqslant 2$.

Results of experiments are presented in Fig. 3. In the regenerative amplification regime, the average radiation power was 13 W at a 3-kHz repetition rate of amplified pulses, which corresponds to a pulse energy of 4.3 mJ. A transverse beam distribution at the output is close to Gaussian, a weak astigmatism is related to the phase profile astigmatism of the disk AE. The long-term stability of the output power was 3% rms. In first experiments, the signal of a fibre master laser stretched

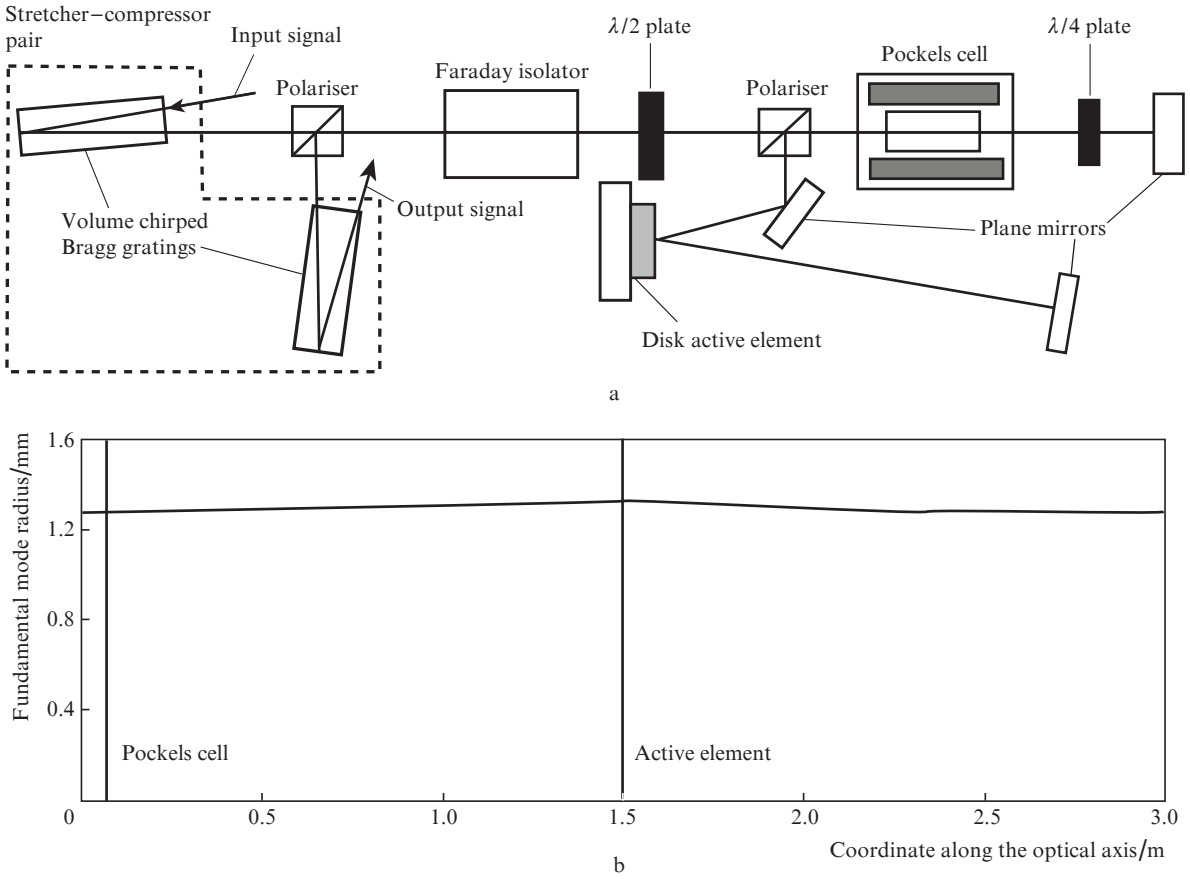

Figure 2. (a) Optical scheme of the regenerative disk amplifier (dashed lines refer to a stretcher–compressor unit planned to be installed) and (b) dependence of a beam radius in the regenerative disk amplifier on the longitudinal coordinate (black vertical lines show the positions of the active element and Pockels cell; the end mirrors of the cavity of the regenerative amplifier are placed at points 0 and 3 m).

to 200 ps with a spectral width of 10 nm passed to a regenerative amplifier where it narrowed to approximately 1 nm in the amplification process. This resulted in shortening its duration to about 20 ps; at this duration, the breakdown threshold of dielectric coatings is $\sim$1 J cm^{-2}. In view of the fact that the beam diameter in the BBO crystal is 2.4 mm, a further increase in the regenerative amplifier output energy may lead to a breakdown of the electro-optical element.

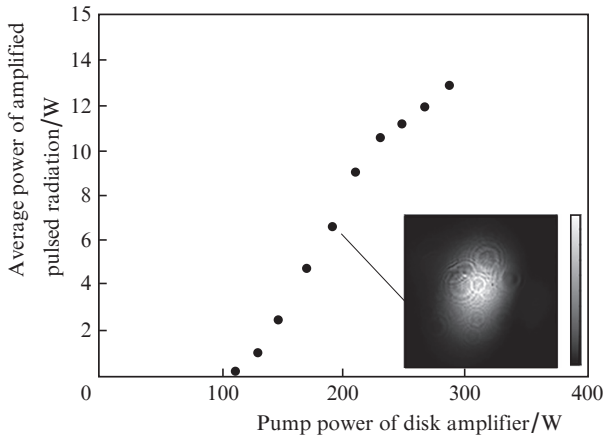

Figure 3. Dependence of the average radiation power at the output from the regenerative amplifier on the average pump power. The inset shows the transverse distribution of the output beam.

Note that a relatively low efficiency of the regenerative amplifier is mainly related to high losses in the electro-optical element (about 0.3% per each crystal face) due to poor quality of antireflection coatings. Now we work on developing a Pockels cell with a BBO crystal possessing the reflecting coatings improved to a loss level of 0.1%, which will increase the differential efficiency to 20%. Note that the laser cavity of the regenerative amplifier was tested in a single-mode oscillation without an electro-optical element; the differential efficiency was 26% at the output power of up to 70 W. To increase the pulse energy, chirped Bragg gratings (Optigrate) at the amplifier input and output will be installed with a dispersion of 190 pc nm^{-1} and aperture 8×8 for stretching the radiation pulses with a bandwidth of 1 nm to 190 ps and following compressing those to 20 ps (see Fig. 2). This approach and a slightly increased diameter of the fundamental mode of the regenerative amplifier will raise the pulse energy to 20 mJ without a breakdown of optical elements. In addition, since the pulses amplified in the regenerative amplifier are synchronised with pulses of a femtosecond system described below, by choosing the amplifier pulse (from a series of pulses with a PRR of 60 MHz) it is possible to minimise the delay between the pulses. According to [15], the expected jitter between the pump pulse and femtosecond pulse is $\sim$1 ps.

We plan to feed part of the regenerative amplifier signal to a second Yb:YAG disk amplifier for increasing the pulse energy. An optical scheme of the multipass amplifier is shown in Fig. 4. The amplified beam of diameter 3 mm passes through a Faraday isolator (*1*) to a disk AE (*2*) of thickness 2.5 mm with a doping level of 3 at.%. Then the radiation reflects successively from several 45° mirrors (*3*) and four times reflects from the AE. For additional four reflections, the radiation is directed to a telescope (*4*) and reflects backward from the second mirror of the telescope. A $\lambda/4$ plate provides polarisation decoupling by extracting radiation reflected from the polariser of the Faraday isolator. Radiation of the diode pumping with a maximal power of 1.1 kW and adjusted pulse duration (of about 1 ms) passes twice across the disk AE. The pump pulse repetition rate may vary up to several hundred Hz.

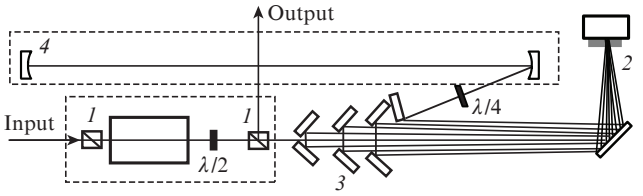

Figure 4. Optical scheme of a multipass disk amplifier: (*1*) Faraday isolator; (*2*) disk active element; (*3*) 45° mirrors of the multipass system; (*4*) telescope.

To minimise thermal effects, first experiments with the multipass disk amplifier were performed at a pump pulse duration of 1.12 ms and PRR of 10 Hz. In future, the PRR will be increased to about 100 Hz. The disk mupltipass amplifier has been tested with an input signal of energy 1.5 mJ stretched to 300 ps. Results of the experiment are presented in Fig. 5. The pulse energy of 70 mJ and gain of above 40 were obtained. A near field transverse beam distribution is close to Gaussian. A further increase in the pump power leads to the breakdown of optical elements in the amplifier, which, probably is related to distortions of the pulse time profile in the saturation regime (pulse rolling) [16].

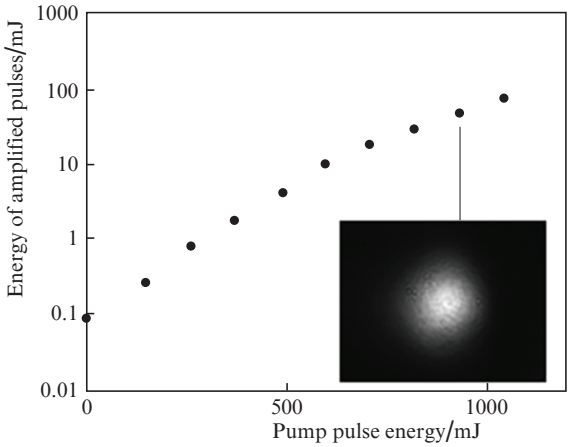

Figure 5. Dependence of the output energy on the pump pulse energy of the multipass amplifier. The inset shows the transverse beam distribution at the amplifier output.

An expected increase in the pulse energy to 200 mJ at the output of the muplipass amplifier will be reached by increasing the input pulse energy from 1.5 to 5 mJ and pump pulse energy to 1.5 J. In particular, this will increase the aperture of an amplified beam from 3.5 to 5 mm and substantially increase the breakdown threshold. Additionally, to suppress the pulse rolling effect, a preliminary time profiling of the laser pulse will be employed (similarly to [17]). For operation at a PRR of 100 Hz, the AE thickness will be reduced to 1 mm and the doping level will be higher.

3. Generation and amplification of a femtosecond signal

The main signal of the sub-picosecond ytterbium laser passes to the channel of femtosecond pulse generation and amplification. First results of this investigation are presented in [18]. An improved scheme of IR femtosecond pulse generation is given in Fig. 6. A signal with the pulse energy of above 0.3 mJ, duration of 250 fs, and PRR tunable up to 15 kHz is directed to a BBO crystal (*1*), where part of the signal energy (~100 μJ) converts to the second harmonic. Then, a dichroic mirror (*2*) separates signals with wavelengths 1030 and 515 nm, and a dichroic mirror (*3*) additionally divides the signal of the second harmonic in the ratio 1:3. The smaller part is focused to a YAG crystal (*4*) for generating supercontinuum in the range of 400–800 nm. The long-wavelength part of the radiation is collimated by a spherical mirror (*5*), selected by the dichroic mirror (*6*), and passes to a nonlinear crystal BBO (*7*) of thickness 1.5 mm. The greater part of the second harmonic signal is directed through a delay line (*8*) to the BBO crystal (*7*) for collinear parametric amplification of the long-wavelength part of supercontinuum in the range of 650–720 nm. Here, a difference frequency radiation is generated in the wavelength range of 1800–2500 nm. According to [19], this radiation has a stable phase between the electromagnetic field and envelope, which is an important advantage in attosecond physics. Then the difference-frequency signal is selected by a dichroic mirror (*9*) and filter (*10*) and passes to a stage of a non-collinear parametric amplification on a BBO crystal (*11*) of thickness 2 mm. Due to a delay line (*12*), the radiation of the fundamental wavelength 1030 nm remained after second harmonic generation passes to the crystal simultaneously. The angle of non-collinear interaction in air is approximately 2°. A diameter of the parametric pump beam is 2 mm at a maximum energy of up to 200 μJ. The pump and signal radiation pass twice through a nonlinear element (*11*) with the same matching angle ($\theta \approx 21.4°$), which substantially increases the conversion efficiency. To extract the radiation, the signal and pump pulses are reflected at a small angle in the vertical plane (orthogonal to the plane of Fig. 6). The matching angle mentioned above provides wideband amplification in BBO in the range of 1800–2500 nm [20].

Measurement results are presented in Figs 7 and 8. All the measurements were taken at the 3-kHz PRR of the regenerative ytterbium amplifier. At the pump pulse energy of 205 μJ the energy of the amplified pulse with a centre wavelength of 2250 nm was 26 μJ at the conversion efficiency of above 12% (Fig. 7). The long-term stability of the average power of amplified radiation was 2% rms. The spectral width of amplified radiation was more than 200 nm with a centre wavelength varied from 1950 to 2250 nm, which corresponds to the transform limited duration of less than 40 fs. The tuning was realised by varying the matching angle of BBO (*7*). Note that in this scheme, the bandwidth of the amplified signal was limited by the matching bandwidth of collinear interaction while generating the difference frequency in the BBO crystal (*7*). A reduction of its thickness from 1.5 mm to 0.5 mm with a small reduction of a diameter of the second-harmonic pump beam will approximately thrice increase the bandwidth of the difference signal spectrum and provide its wideband amplification in the range of 1900–2400 nm.

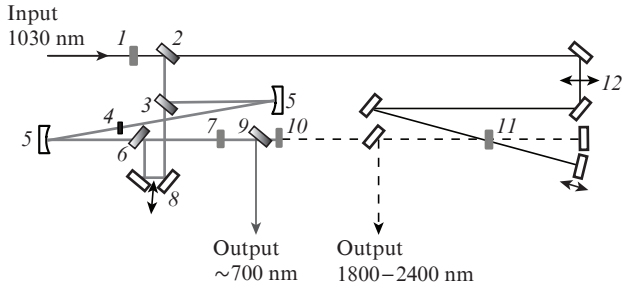

Figure 6. Optical scheme for femtosecond pulse generation and parametrical amplification (black lines show radiation with a wavelength of 1030 nm, grey lines refer to radiation in the visible and near-IR ranges, dashed lines refer to radiation in the range of 2 μm):
(*1*, *7*, *11*) BBO crystals; (*2*, *3*, *6*, *9*) dichroic mirrors; (*4*) YAG crystal; (*5*) spherical mirrors; (*8*, *12*) delay lines; (*10*) filter IKS.

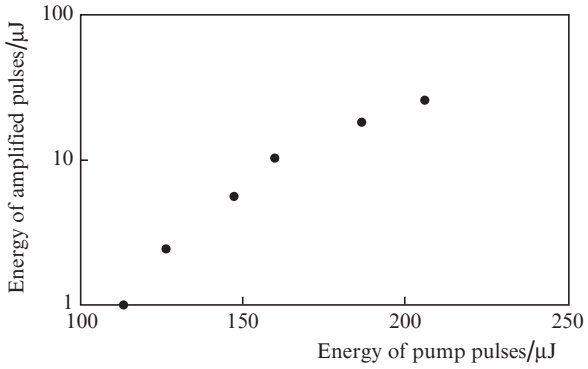

Figure 7. Dependence of the energy of amplified femtosecond pulses with a centre wavelength of 2250 nm on the pump pulse energy.

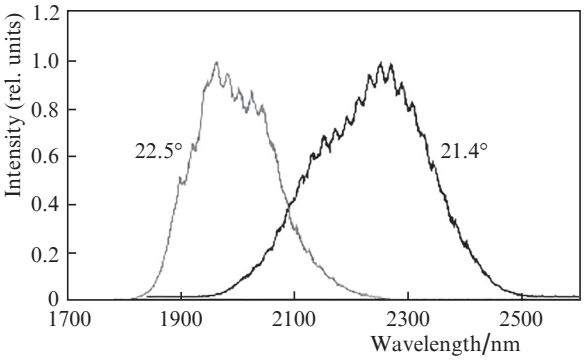

Figure 8. Spectral distribution of the intensity of amplified femtosecond pulses at the BBO crystal (*7*) matching angles $\theta = 21.4°$ and 22.5°.

Unfortunately, the range of wavelengths longer than 2 μm is difficult for studying transverse and temporal distributions of the pulse. In the scheme from [18] akin to that described above, the compression of a femtosecond pulse with a centre wavelength of 1.4 μm to a duration of 30 fs was investigated. In the present work, the compression of amplified femtosecond pulses to a transform limited duration has also been studied. The measurements were performed with a commercial device based on the SHG-FROG approach [21]. A spectral sensitivity of this device was limited by a wavelength of

2100 nm due to a sharp fall in the spectral sensitivity of the employed CCD array at $\lambda > 1050$ nm. Thus, femtosecond radiation pulses were studied in a shorter-wavelength range at $\theta = 22.5°$ (see Fig. 8), in which case the radiation band is narrower. According to the measurement taken, the employment of a 4-mm-thick ZnSe plate (which has the group velocity dispersion of approximately 300 fs^2 mm^{-1}) provided compression of radiation pulses from 100 to 50 fs at the pulse transform limited duration of 40 fs (Fig. 9). The error of the FROG algorithm was 2.1%. One may expect that a radiation pulse with the spectrum corresponding to the angle $\theta = 21.4°$ can be compressed to a duration shorter than 40 fs.

Further amplification of a femtosecond signal at the wavelength of ~2 μm to the millijoule energy range requires the employment of the chirped pulse amplification method [22], which allows one to minimise various nonlinear effects arising in pulse propagation both in air and in gain media. In the framework of the present work, two experimental realisations of femtosecond pulse stretching and compression are considered for a next-stage parametric amplification under the pumping by 30-ps pulses of a regenerative amplifier.

1. The employment of a classical stretcher and compressor with a 10–15 ps chirp and non-collinear OPCPA scheme based on a BBO crystal. This problem can be solved by using a Martinez [23, 24] or Offner [25] stretcher based on commercially available diffraction gratings (DGs) (Thorlabs) of size 50×50 mm ruled with 600 lines mm^{-1}. By using a spherical mirror with a focal length of 200 mm combined with a plane mirror one can build a compact single-grating stretcher with a characteristic size of 250×100 mm and varied duration of output radiation in a required range of 10–20 ps. Unfortunately, a small dispersion prevents the employment of a classical Treacy compressor scheme [26], in which, according to calculations, a distance between the DGs is 1–2 cm. A grating compressor based on a similar DG can be assembled similarly to the stretcher, with the DG shifted to opposite direction along the optical axis of the system. An advantage of such a pair is a possibility to exactly match the dispersions of the stretcher and compressor and to adjust the compressor dispersion for compensating the phase incursion in the amplifier. At a femtosecond pulse energy of up to 1 mJ, one can avoid the breakdown by using a magnifying telescope. Drawbacks are poor optical damage threshold of the grating and high compressor losses (~35%), which is important for further system scaling with a more high-power pump source. As an alternative, the compression due to the employment of dispersion in various glasses can be used. This will help avoid the drawbacks mentioned above and, however, will require matching higher-order dispersions between the stretcher and compressor.

2. An alternative to the first variant is the method of high gain frequency domain optical parametric amplification (FOPA) [27]. Comparison of this approach with classical parametric amplification of chirped pulses is thoroughly described in [28]. The main advantages of the new method are a combined stretcher–compressor system with perfect dispersion matching in a single scheme with an amplifier, and absence of requirement on pulse time profiling for homogeneous amplification over the entire spectral range. In our case, in experiments, it is more convenient to employ the modification of this scheme with cylindrical mirrors rather than spherical [5]; the DG ruled with 600 lines mm^{-1} mentioned above is the most appropriate for pulse stretching to the duration of ~15 ps inside the amplifier. However, due to a greater divergence angle of the radiation reflected from the DG, a number of difficulties arise in designing an optical scheme for the amplifier. In addition, parametrical amplification requires a BBO crystal with a rather large aperture ($\sim 10 \times 25$ mm). Up to now, several variants are calculated for performing preliminary experiments; the final decision will be formulated issuing from the results obtained.

Taking into account the results of realised variants of chirped femtosecond pulse amplification described above, the next stage of the parametrical amplifier will be developed under pumping by the radiation pulses with an energy of up to 200 mJ from the output of a multichannel disk amplifier. If necessary, the radiation after the multipass amplifier can also be compressed to a duration of several tens of picoseconds. As a result, at the conversion efficiency of above 10%, the energy of femtosecond pulses may increase to 30 mJ, and after compression to a transform limited duration the peak power may reach 1 TW, which is close to the record values in the IR range for today.

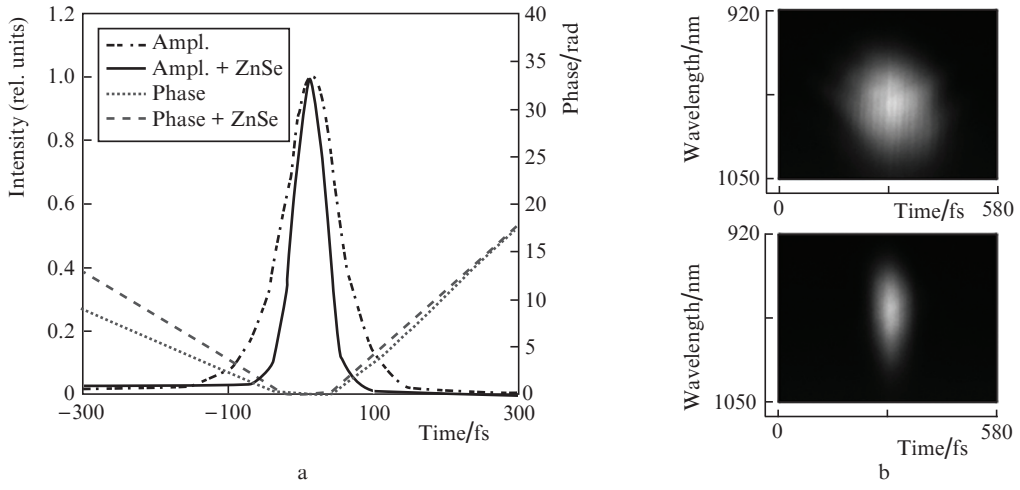

Figure 9. (a) Time dependence of the pulse intensity and phase, recovered by the FROG method and (b) spectral and temporal distributions of the intensity in pulse duration measurements (top) before and (bottom) after compression with the employment of a ZnSe plate.

4. Conclusions

The work presents first results of developing a laser system with a centre wavelength in the range of 2 μm based on modern approaches to generation and amplification of femtosecond pulses and production of picosecond ytterbium lasers. A femtosecond radiation channel provides a pulse energy of above 20 μJ at a wavelength in the range of 1.9–2.4 μm. Such a spectral width of the gain corresponds to the transform limited duration of less than 2 fs. Here, passive phase stabilisation is realised between the electromagnetic field and its envelope (CEP stabilisation). The pump channel based on a regenerative disk amplifier was synchronised with the femtosecond radiation and provided an output energy of up to 5 mJ at a pulse duration of ~20 ps and pulse repetition rate of 3 kHz. For pumping the next stage, a multipass disk amplifier is developed; the first experimental study of the latter demonstrated an output pulse energy of 70 mJ. In addition, a principal design of the next parametric amplification stage is developed.

The laser system with an energy level of 20 μJ and centre wavelength in the range of 2 μm can be employed in scientific research in ultrafast laser spectroscopy and certain investigations in attosecond physics. As a next step, the signal energy will be increased to a millijoule level by using 20-mJ pump pulses of a regenerative amplifier optically matched with the femtosecond system elaborated. In addition, approaches to obtaining amplified pulses with a terawatt peak power will be developed by using a multipass disk amplifier as a source of pump pulses.

Acknowledgements. The work was supported by the Presidium of the Russian Academy of Sciences (Fundamental Research Programme 'Extreme Light Fields and Their Interaction with Matter', Project No. 0035-2018-0023) in part of the development of a femtosecond source with a centre wavelength of ~2 μm. The work was also supported by the Ministry of Education and Science of the Russian Federation (Project No. 075-15-2019-1371, unique identifier RFMEFI60718X0201) in part of the development of ytterbium pump lasers.

References

1. Gaumnitz T., Jain A., Pertot Y., Huppert M., Jordan I., Ardana-Lamas F., Wörner H. *J. Opt. Express*, **25**, 27506 (2017).
2. Jahn O., Leshchenko V.E., Tzallas P., Kessel A., Krüger M., Münzer A., Trushin S.A., Tsakiris G.D., Kahaly S., Kormin D., Veisz L., Pervak V., Krausz F., Major Z., Karsch S. *Optica*, **6**, 280 (2019).
3. Woodbury D., Feder L., Shumakova V., Gollner C., Schwartz R., Miao B., Salehi F., Korolov A., Pugžlys A., Baltuška A., Milchberg H.M. *Opt. Lett.*, **43**, 1131 (2018).
4. Clerici M., Peccianti M., Schmidt B.E., Caspani L., Shalaby M., Giguère M., Lotti A., Couairon A., Légaré F., Ozaki T., Faccio D., Morandotti R. *Phys. Rev. Lett*., **110**, 253901 (2013).
5. Gruson V., Ernotte G., Lassonde P., Laramée A., Bionta M.R., Chaker M., Di Mauro L., Corkum P.B., Ibrahim H., Schmidt B.E., Legaré F. *Opt. Express*, **25**, 27706 (2017).
6. Fu Y., Nishimura K., Suda A., Midorikawa K., Takahashi E. *Proc. SPIE LASE*, **10522** (2018).
7. Baumgarten C., Pedicone M., Bravo H., Wang H., Yin L., Menoni C.S., Rocca J.J., Reagan B.A. *Opt. Lett*., **41**, 3339 (2016).
8. Jung R., Tümmler J., Will I. *Opt. Express*, **24**, 883 (2016).
9. Budriûnas R., Stanislauskas T., Varanavičius A. *J. Opt*., **17**, 094008 (2015).
10. Alismail A., Wang H., Altwaijry N., Fattahi H. *Appl. Opt*., **56**, 4990 (2017).
11. Volkov M.P., Kuznetsov I.I., Mukhin I.B., Palashov O.V. *Quantum Electron*., **49**, 354 (2019) [*Kvantovaya Elektron*., **49**, 354 (2019)].
12. Saltarelli F., Koenen D., Lang L., Graumann I.J., Phillips C.R., Keller U. *Proc. Laser Congress* (Vienna, OSA, 2019) p. JM5A.35.
13. Volkov M.R., Mukhin I.B., Kuznetsov I.I., Palashov O.V. *J. Opt. Soc. Am. B*, **36**, 1370 (2019).
14. Diebold A., Saltarelli F., Graumann I.J., Saraceno C.J., Phillips C.R., Keller U. *Opt. Express*, **26**, 12648 (2018).
15. Casanova A., D'Acremont Q., Santarelli G., Dilhaire S., Courjaud A. *Opt. Lett*., **41**, 898 (2016).
16. Schimpf D.N., Ruchert C., Nodop D., Limpert J., Tünnermann A., Salin F. *Opt. Express*, **16**, 17637 (2008).
17. Mironov S.Y., Poteomkin A.K., Gacheva E.I., Andrianov A.V., Zelenogorskii V.V., Vasiliev R., Smirnov V., Krasilnikov M., Stephan F., Khazanov E.A. *Laser Phys. Lett*., **13**, 055003 (2016).
18. Mukhin I.B., Kuznetsov I.I., Palashov O.V. *Quantum Electron*., **48**, 340 (2018) [*Kvantovaya Elektron*., **48**, 340 (2018)].
19. Baltuška A., Fuji T., Kobayashi T. *Phys. Rev. Lett*., **88**, 133901 (2002).
20. Lai C.-J., Hong K.-H., Siqueira J., Krogen P., Chang C.-L., Stein G., Liang H., Keathley P., Laurent G., Moses J., Zapata L., Kärtner F. *J. Opt*., **17**, 094009 (2015).
21. DeLong K.W., Trebino R., Hunter J., White W.E. *J. Opt. Soc. Am. B*, **11**, 2206 (1994).
22. Strickland D., Mourou G. *Opt. Commun*., **56**, 219 (1985).
23. Martinez O. *IEEE J. Quantum Electron*., **23**, 59 (1987).
24. Fiorini C., Sauteret C., Rouyer C., Blanchot N., Seznec S., Migus A. *IEEE J. Quantum Electron*., **30**, 1662 (1994).
25. Offner A. Patent US No. 3748015 (priority date July 24, 1973).
26. Treacy E.B. *IEEE J. Quantum Electron*., **QE-5**, 454 (1969).
27. Schmidt B.E., Thiré N., Boivin M., Laramée A., Poitras F., Lebrun G., Ozaki T., Ibrahim H., Légaré F. *Nat. Commun*., **5**, 3643 (2014).
28. Lassonde P., Thiré N., Arissian L., Ernotte G., Poitras F., Ozaki T., Larameé A., Boivin M., Ibrahim H., Légaré F., Schmidt B.E. *IEEE J. Sel. Top. Quantum Electron*., **21**, 1 (2015).